Antarctic Science 21(4), 373–382 (2009) © Antarctic Science Ltd 2009 doi:10.1017/S0954102009002028

Deglaciation and weathering of Larsemann Hills, East Antarctica

KEVIN KIERNAN[1]*, DAMIAN B. GORE[2], DAVID FINK[3], DUANNE A. WHITE[2], ANNE McCONNELL[1] and INGVAR A. SIGURDSSON[4]

[1]*School of Geography & Environmental Studies, University of Tasmania, Private Bag 78, TAS 7001, Australia*
[2]*Department of Environment & Geography, Macquarie University, NSW 2109, Australia*
[3]*Environment Division, ANSTO, Menai, NSW 2234, Australia*
[4]*South Iceland Nature Centre, Strandvegur 50, 900 Vestmannaeyjar, Iceland*
**Kevin.Kiernan@utas.edu.au*

Abstract: *In situ* cosmogenic ^{10}Be exposure dating, radiocarbon determinations, salt and sediment geochemistry, and rock weathering observations indicate that parts of Larsemann Hills, East Antarctica have been subaerially exposed throughout much of the last glacial cycle, with the last glaciation occurring prior to 100 ka BP. Salt-enhanced subaerial weathering, coupled with a paucity of glacial erratics, made exposure age dating challenging. Rapid subaerial surface lowering in some places means that some exposure ages may underestimate the true age of deglaciation. Despite this uncertainty, the data are consistent with the absence of overriding by a thick ice sheet during the Last Glacial Maximum ~20–18 ka BP.

Received 3 September 2008, accepted 9 February 2009

Key words: Broknes, cosmogenic nuclide exposure age, mumiyo, salt geochemistry, Stornes

Introduction

The ice free oasis of Larsemann Hills (69°23'S, 76°53'E), on the Prydz Bay coast of East Antarctica comprises two main peninsulas, Broknes and Stornes, which together total ~40 km^2 (Fig. 1). Exposure of Broknes through the last glacial cycle has been suggested on the basis of lake cores radiocarbon dated to > 44 ka BP and underlying presumed interglacial sediment indicative of conditions several degrees warmer than the present (Hodgson *et al*. 2001, 2005, 2006, Squier *et al*. 2005, Cromer *et al*. 2006). However, while these lacustrine sediments have been suggested to date from the last interglacial *c.* 120 ka BP, a firm chronology has not yet been provided nor has the stratigraphy been described sufficiently well to demonstrate a continuous and uninterrupted sedimentary sequence. Hence, the possibility remains that the interglacial material is of much greater age and that a break in sedimentation or even an erosional unconformity exists between the "interglacial" sediments and the younger sediments successfully dated using radiocarbon.

The age of the last deglaciation of Larsemann Hills remains unclear. Gillieson (1991) argued that the area was covered by a few hundred metres of ice during the last global glacial maximum (global LGM), offshore islands become ice free at ~9.5 ka and the last deglaciation occurred only at ~4.5 ka. Subsequently, a date of 24 950 ± 710 ^{14}C yr BP (ANU 8826; Burgess *et al.* 1994) from moss buried at 2.5 m depth in sediments on the northern shore of Lake Nella, only 2 km from the present edge of the ice sheet on Broknes, showed that this part of Larsemann Hills was ice-free during the global LGM. More recently, accelerator mass spectrometry radiocarbon ages of biogenic material from lake cores and an optically stimulated luminescence age from a glaciofluvial deposit, led Hodgson *et al.* (2001) to conclude that parts of Broknes had been ice free since at least 44 ^{14}C ka BP. In contrast, nearby Stornes is believed to have deglaciated during the mid–late Holocene (Hodgson *et al*. 2005, Squier *et al*. 2005).

Both bedrock and surficial sediments are strongly weathered in many parts of Larsemann Hills. Salt weathering is the key process causing rock breakdown, and the finer weathering products are removed by the wind leaving a lag of larger fragments, and facilitating erosion of rock surfaces downwind by saltating grains. However, there are distinct variations in the intensity of rock weathering, particularly on Broknes, where well-developed tafoni pits and evidence of areal lowering of rock surfaces are conspicuous. These weathering features are best developed in northern and eastern Broknes and on Mirror Peninsula (an eastern extension of Broknes). The north-eastern weathered zone is demarcated from the south-west of Broknes by a diffuse boundary which is oriented ESE–WNW across the peninsula. It is unclear whether this boundary is related to age of exposure (and thus glacial history) or a zone of weathering enhancement due to dispersal of sea salt.

Micro-erosion meter measurements from the strongly weathered area of Broknes north and east of Lake Nella (Fig. 1) over a six year period, showed annual surface lowering of *c.* 0.015 mm yr^{-1} (Spate *et al.* 1995). The data show both surface lowering via periodic detachment of single grains, and a steady rate of lowering such as might occur through wind-assisted abrasion by saltating grains. Salts such as halite (NaCl) and particularly thenardite (Na_2SO_4), which precipitate as a consequence of the evaporative concentration of seawater, enhance rock weathering (e.g. Williams &

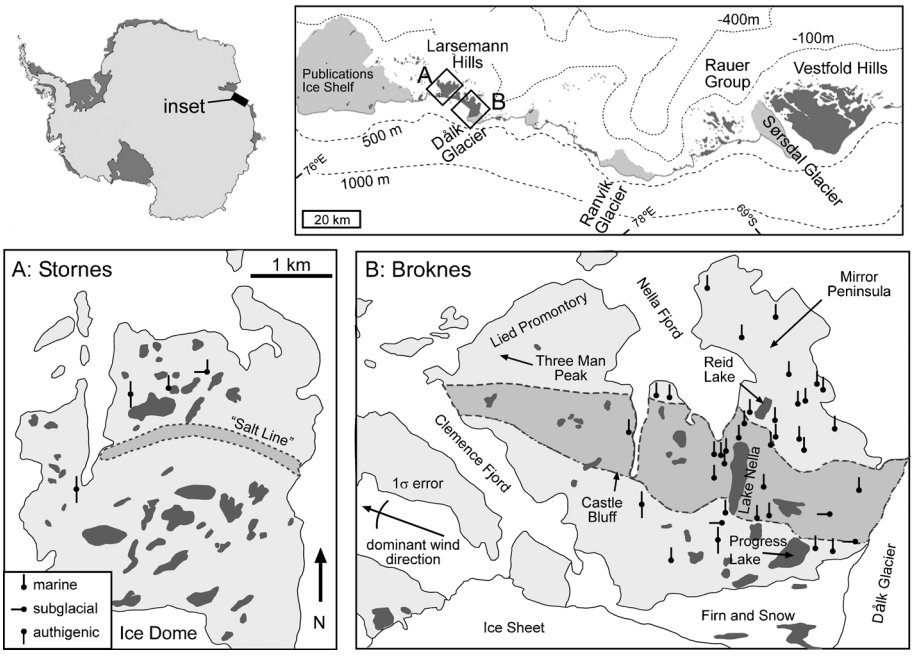

Fig. 1. Larsemann Hills, the distribution of types of salt minerals and the location of the "salt line". The "salt line", revealed by the salt (Supplementary Table III - see www.journals.org/jid_ANS), sediment chemistry (Supplementary Table IV - see www.journals.org/jid_ANS) and field observations of rock weathering, lies downwind of the marine inlets. The maximum monthly wind direction (over 59 months) is represented by an arrow; the error bar shows ± 1 SD.

Robinson 1981, Jerwood *et al*. 1990, Sumner 2004) and the dominant ESE wind direction across Larsemann Hills (Bien *et al*. 1994) provides an effective mechanism for dispersal of sea spray.

This study has three aims. First, it applies cosmogenic nuclide dating with ^{10}Be to assess critically the proposition that Broknes was deglaciated at or prior to the Last Interglacial, using terrestrial cosmogenic nuclide exposure ages which allow age determinations beyond the range achievable using radiocarbon. Second, due to the apparent disparity in deglaciation ages between the peninsulas, it re-examines the notion of Holocene emergence of Stornes from the ice. Third, the study explores rock weathering, chemistry of sediment:water extracts and the mineralogy of salt efflorescences in order to determine whether the observed patterns represent former glacial limits or simply salt-enhanced weathering. Mumiyo, the layered deposits of proventricular oil ejected by snow petrels (*Pagodroma nivea* Forster) as a defensive mechanism against predation, was radiocarbon dated in order to gain insights into the minimum ages of rock weathering features within which nesting has occurred.

Field area

Larsemann Hills is a Proterozoic terrain consisting of a layered complex of cordierite- and iron–titanium-rich gneiss, leucogneiss and a dominant heterogeneous migmatitic paragneiss composed of discontinuous lenses of metapelite with abundant sillimanite, spinel, cordierite, garnet, K-feldspar and biotite (Stuwe *et al*. 1989, Dirks *et al*. 1993, Carson *et al*. 1995). The two main peninsulas - Broknes to the east and Stornes to the west - are different in that the former is largely free of ice and snow whereas the latter is largely snow covered, and hosts an ice dome 4.9 km^2 in area and 170 m altitude (Gore 1997). Hill summits reach 170 m above sea level, with the highest terrain occurring near the ice edge. The peninsulas are deeply dissected by short (up to 1 km) valleys that have formed along structural lineaments, particularly joints, in response to erosion by ice and water. In winter mean monthly air temperatures are -18°C to -15°C but in summer (December–February) temperatures above +4°C are common and sometimes reach +10°C. Annual precipitation, received as snow, is probably no more than 250 mm water equivalent. On most mornings the hills are swept by strong katabatic winds from the ice sheet. The dominant direction of strong winds is ESE (100 ± 20°, $n = 59$; wind data in Bien *et al*. 1994), providing an effective mechanism for dispersal of sea spray onto parts of the peninsulas downwind of the marine inlets (Fig. 1).

Methods

Rock weathering

Measurements of weathering and erosion of sediments and bedrock surfaces were undertaken to constrain the relative age of the landforms and sediments. Parameters measured were the depth and continuity of weathering pits, depth of boulder surface recession relative to remnant tafoni protrusions, and the lithological composition of glacial sediments in the intense weathering environment above the present ground surface in comparison to that of the immediately subjacent till where weathering is less intense. Comparisons were drawn between the studied sites and the weathering status of surfaces below the limit of Holocene marine transgression from which

https://doi.org/10.1017/S0954102009002028 Published online by Cambridge University Press

weathering features are likely to have been abraded by marine action and shore ice, to some extent resetting the weathering surface at a known time.

Chemistry of sediment and salt efflorescences

A ~200 g sample of surficial sediment was collected from a grid with a 0.5 ± 0.2 km spacing. Samples of solutes were extracted by slow rolling 10 g of sample and 50 ml of deionised water in glass tubes for 2.5 h and then centrifuged at 3000 rpm for 10 minutes. Conductivity was determined using a Radiometer CDM 80 conductivity meter. Analyses of sodium, potassium, calcium and magnesium were performed on a GBC Scientific Equipment Double Beam flame atomic absorption spectrometer model 902. Chloride was measured using a Radiometer ION 85 Ion analyser with a F1012Cl chloride electrode and a double bridged K701 calomel reference electrode. Salt efflorescences, collected from bedrock and sediment surfaces, were examined using a JSM 35C scanning electron microscope to assess surface morphology and determine approximate elemental composition. Specimens were mounted on thick pyrolytic graphite substrates using conducting carbon paint. Fluorescent X-rays emitted from the sample were analysed using a Tracor 2000 electron probe microanalysis system to determine approximate atomic composition. This technique cannot be used to detect elements with atomic numbers less than fluorine, precluding measurement of carbon or oxygen. Electron photomicrographs of selected samples were taken. Efflorescences with sufficient mass were also examined using X-ray diffractometry (XRD), to identify the dominant minerals. Samples were finely ground under acetone using an agate mortar and pestle, and mounted on glass plates. The XRD data were acquired using a GBC Scientific Equipment diffractometer with CuK_{α} radiation. Diffractograms were acquired over 5–65° 2θ with generator at 35 kV and 1 kW, and instrument settings of 0.02° step size, 1.2 s per step, 1.0 mm divergence slit, 0.2 mm receiving slit, 1.0 mm soller slit, and with spinning stage operational. PANalytical High Score Plus software v. 2.2 was used with the International Center for Diffraction Data minerals subfile, and mineral identifications were coded definite, highly probable or probable according to the goodness of fit of the X-ray reflections.

^{14}C dating of mumiyo

Mumiyo samples were obtained from nesting sites at 75–100 m altitude on the north-western slopes of Three Man Peak at the seaward tip of Broknes, 3.3 km from the present margin of the ice sheet (Fig. 1). The nests were in tafoni hollows or crevices between angular fragments of dislodged bedrock. The basal 2 mm of each mumiyo deposit was dated in order to identify the earliest date of nest occupation and determine a minimum age for the weathering feature. Analyses were performed using the Australian National Tandem Accelerator for Applied Research (ANTARES) at the Australian Nuclear Science and Technology Organisation (ANSTO; Lucas Heights, Australia; Fink *et al*. 2004).

Exposure age dating

Sampling for exposure age dating was complicated by a paucity of glacial erratics. Exposure age dating programs in formerly glaciated environments typically aim to sample erratics which have had continuous subaerial exposure since initial release from the ice sheet or glacier. Since glacial erratics were largely absent, only abraded bedrock surfaces were sampled. Unfortunately, strongly weathered rock surfaces are widespread, and the degree and pattern of rock surface disintegration created considerable difficulty for the sampling of minimally weathered rock surfaces. Samples were obtained from rare slabs of glacially abraded rock adjacent to surfaces that retained residual glacial polish or, in rare cases, glacial striae. Because striated surfaces were rare, we sampled the ice abraded surfaces immediately adjacent to the striae (for geoconservation reasons). Sites were selected that were unlikely to have been sediment sinks or subject to deep burial by accumulated snow. On Broknes, three samples were obtained from near the outlet to Lake Nella, close to the sediments dated to ~25 ka BP (Burgess *et al*. 1994), and from four sites between Castle Bluff (~120 m a.s.l.) and the northern extremity of the peninsula. Six sites at varying altitudes (~40–110 m) and distances from the coast were sampled on Stornes. Quartz was isolated from the samples using the procedure of Child *et al*. (2000), and cosmogenic ^{10}Be concentrations measured at the ANTARES facility at ANSTO using the method outlined by Fink & Smith (2007).

Due to our selection of bedrock sites immediately adjacent to the striae, it is probable that subaerial weathering and erosion following deglaciation has reduced the ^{10}Be concentration (and hence apparent age) of our samples when

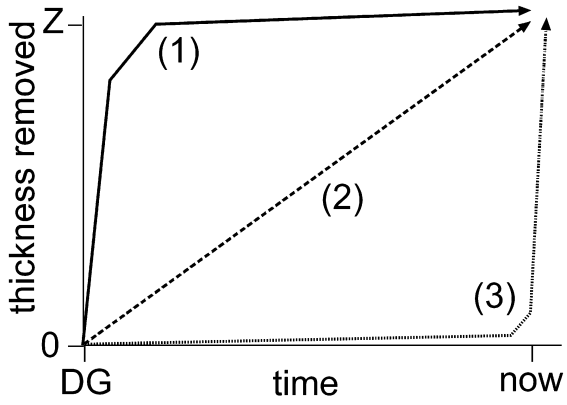

Fig. 2. Scenarios used to correct cosmogenic ages for subaerial erosion. Z = total erosion thickness, indicated by height difference between sampled surfaces and striated surfaces nearby, DG = deglaciation. (1–3) mark scenarios as described in text.

https://doi.org/10.1017/S0954102009002028 Published online by Cambridge University Press

compared to the nearby striated surfaces. Therefore, we corrected these ages for erosion using the vertical distance between these surfaces. It is unlikely that weathering and erosion has occurred at a linear rate since deglaciation, hence, we have provided boundaries for temporal variations in the rate of post-exposure rock breakdown by presenting modelled ages based on three scenarios (Fig. 2). This approach is also critical for taking account of the possibility of ^{10}Be inheritance, a possibility that precludes relying on the oldest date and assuming that younger dates reflect only greater post-exposure loss of rock mass and the ^{10}Be it contained. Research over the past decade has highlighted the potential for inheritance to give rise to excessively old cosmogenic isotope exposure-age dates in Antarctica (Zwartz 1995, Sugden *et al*. 2005, White 2007). Scenario (1) is where all of the inferred subaerial erosion occurred rapidly following deglaciation. In this scenario, the "new" surface was formed by subaerial erosion very soon after the ice sheet retreated, so it has had a similar amount of time to accumulate ^{10}Be as would be the case had no subaerial erosion occurred. Thus, even if the amount of subaerial erosion was large, no correction is warranted. Scenario (2) is where the inferred erosion occurred at a constant rate over time. This correction is difficult to solve analytically, so it was calculated using an iterative algorithm to obtain the appropriate erosion rate. This iterative solution relies on the knowledge that the erosion rate (ε) can be calculated from the amount of erosion known to have occurred (Z) and the time since deglaciation (t) by:

$$\varepsilon = \frac{Z}{t}$$

While we do not *a priori* know *t*, by substituting for ε in the nuclide production equation (Lal 1991) we can derive a relationship between N (which has been measured) and the true exposure time, and numerically solve for t using least-squares iteration:

$$N = \frac{P\left(1 - e^{-(t\lambda + \mu Z)}\right)}{\lambda + \frac{\mu Z}{t}}$$

Where N = the measured ^{10}Be concentration, μ = the adsorption coefficient, P = the local (surface) ^{10}Be production rate and λ = the decay constant. Lastly, scenario (3) represents instantaneous erosion just prior to sampling, which dictates the maximum possible erosion correction. In this case, for the purposes of the calculation we can assume that no erosion has occurred during the exposure period, but that the measured surface has effectively been shielded by the thickness of rock recently eroded (i.e. Z), which can be calculated using:

$$N = e^{-\mu Z}\frac{P\left(1 - e^{-(\lambda + \mu\varepsilon)t}\right)}{\lambda + \mu\varepsilon}$$

Finally, since we only have results for one isotope, we cannot exclude the possibility of complex exposure histories for any of these samples. In particular, it is possible that some of the ^{10}Be measured in these surfaces was inherited from a period of exposure prior to the glacial event that formed the striations, so the erosion corrected ages provide a maximum exposure age at any site. Should more than one age at one geographic locality be measured, we consider the younger age to be more representative of the period of exposure since the striating event. Also, due to the potential for blanketing by non-erosive ice or thick snow accumulations (e.g. Gore 1997) the ages record the duration of surface exposure since the striating event rather than the absolute chronological time.

Results

Rock weathering

Pronounced rock weathering features occur on both bedrock and surficial sediments in many parts of Larsemann Hills. Some rock types are strongly weathered, contrasting with limited weathering of more resistant rocks even where they are closely juxtaposed. However, broad spatial trends are readily discernible. Minimally weathered rocks occur along the coast within ~4 m of present sea level. On north-western Broknes, cobbles and bedrock surfaces around a small raised beach are little weathered within ~4 m of sea level. Tafoni is only slightly more developed up to ~10 m altitude suggesting that these weathering features have developed since the Holocene marine transgression. Little weathering is evident in valley bottoms close to the Stornes ice dome (Fig. 1). Weathering pits are generally no more than 1–2 mm diameter and are generally absent within 5 m of the valley floors. Similarly, on the floor of a valley ~500 m north of the ice dome, freshly-abraded rock surfaces appear only recently exposed from beneath the ice. These observations suggest little if any survival of weathering features formed prior to the most recent advance of the ice.

More severe weathering of rock surfaces and sediments is evident above ~10 m altitude over most of Stornes and Broknes. Tafoni hollows up to 1.5 m deep and over 2 m long occur on some outcrops. The gruss weathered from the tafoni hollows accumulates locally, although some is removed by wind and in some valley bottoms accumulations of sand and very fine gravel are evident. Projections of the original surface across the tafoni indicate that some glacial boulders of yellow gneiss on the Lake Nella moraines have lost 50–60% of their original volume, while remnant basal plates from boulders that have suffered near-total volume loss are also present. The majority of the ground surface here is covered by gravel and sand-sized material, with analysis of two quadrats giving mean results of 53% for fragments of less than 0.5 cm calibre, 20% for both the 0.5–30 and 30–100 cm classes, and 15% for clasts of > 1 m size. Comparison between the surface and subsurface till clasts reveals that some lithologies have been entirely weathered and eroded from the surface. Some subsurface

https://doi.org/10.1017/S0954102009002028 Published online by Cambridge University Press

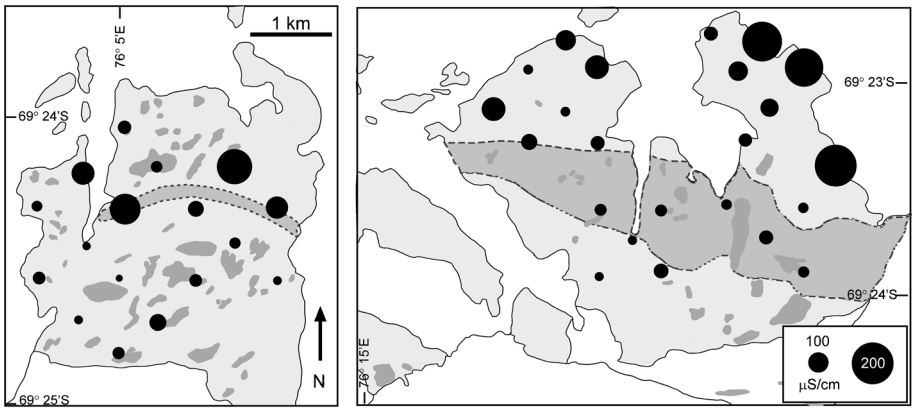

Fig. 3. Conductivity ($\mu S\,cm^{-1}$) of 1:5 sediment:water extracts from Stornes (left) and Broknes (right).

clasts retain a degree of glacial rounding but the surface clasts are generally more angular. A finer grained soil B horizon is also present, despite the likelihood that subsurface weathering rates are slow in this environment. This degree of weathering is vastly greater than that evident below the limit of Holocene marine transgression and implies that the moraines and adjacent rock surfaces are very much older than the Holocene. It also highlights the probability that considerable volumes of cosmic-ray irradiated rock may have been lost from rock surfaces since deglaciation.

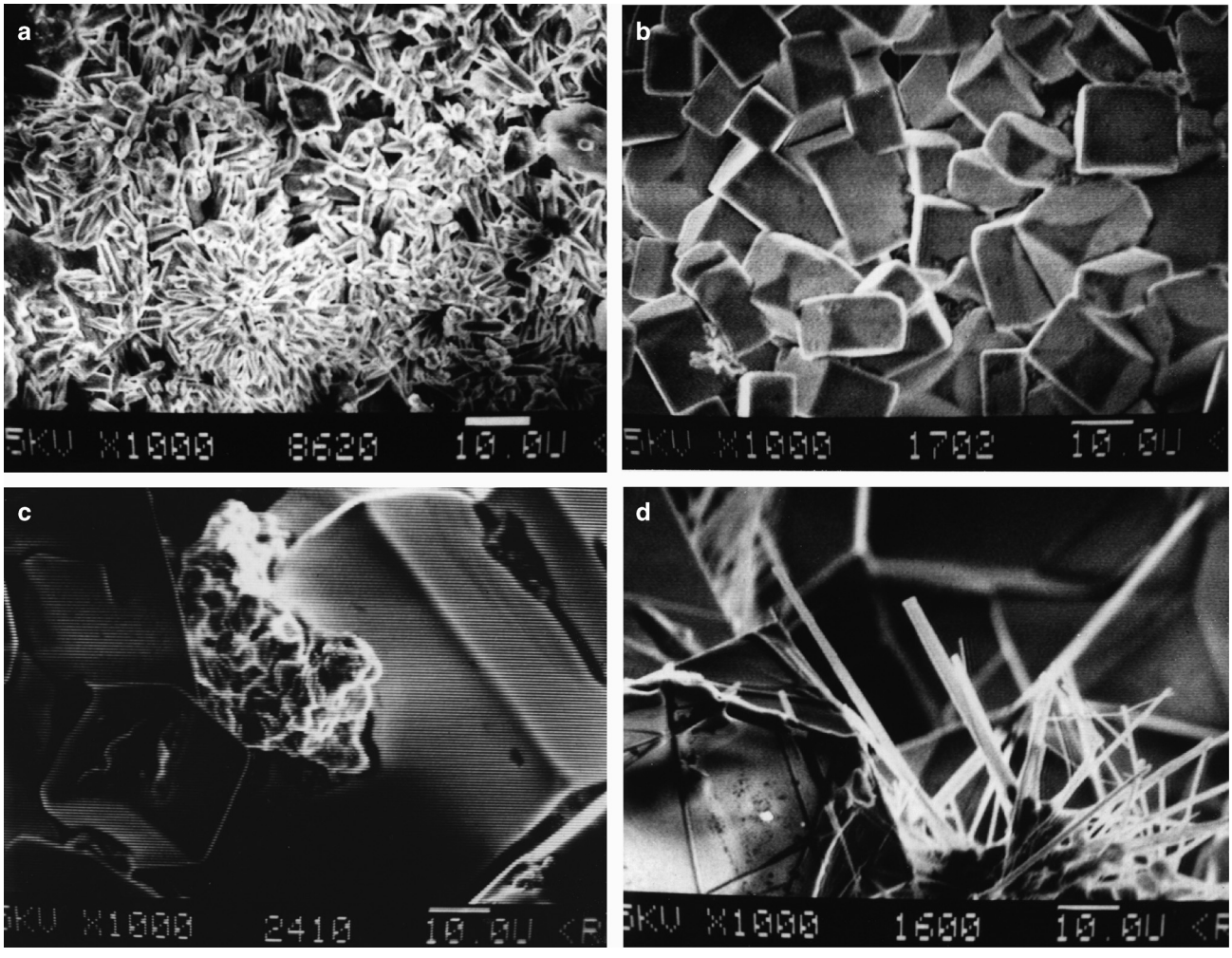

Fig. 4. Representative salt minerals. **a.** Top left: flowers of gypsum ($CaSO_4.2H_2O$). **b.** Top right: cubic crystals of halite (NaCl). **c.** Bottom left: amorphous gypsum nestled between cubic halite crystals. **d.** Bottom right: acicular thenardite (Na_2SO_4) with cubic halite. These samples are from Broknes, and the scale bar on each photomicrograph is 10 µm.

https://doi.org/10.1017/S0954102009002028 Published online by Cambridge University Press

Table I. Mumiyo ^{14}C ages from the Three Man Peak area, Broknes.

Field code	Grid reference	Aspect	Altitude (m)	Thickness (cm)	δ (^{13}C) per mil	% modern carbon pMC	% modern carbon ± 1σ error	^{14}C age (years BP) ± 1σ error	Laboratory code
LHM1	506 027	SE	75	5.0	-30.62	82.89	1.00	1550 ± 100	OZD835
LHM2	507 028	SW	85	10.0	-30.14	80.16	0.63	1820 ± 70	OZD836
LHM3	507 028	NW	100	10.0	-31.44	78.13	0.44	2440 ± 50	OZD837
LHM4a	507 028	NW	85	4.5	-29.31	73.31	0.73	2530 ± 80	OZD838
LHM4b	507 028	NW	85	4.5	-28.10	71.37	0.74	2740 ± 90	OZD839

The most strongly weathered surfaces occur on northern Broknes and on the summits of its highest hills. A rock bench at ~80 m altitude on Lied Promontory (Fig. 1) is strongly etched with little unweathered rock exposed. Talus at least 1.5 m thick occurs on the southern side of Three Man Peak overlooking this bench. Rock surfaces at ~65 m altitude ~1.5 km further south are also well weathered although residual abraded surfaces and rare striae remain locally. The summit area of Castle Bluff (~115 m altitude) exhibits many small pans and pronounced tafoni with hollows up to 2 m deep, 4 m long and 1.8 m wide. Weathering along joints has produced features visually similar to karstic grikes that are incised up to 3 m below surrounding outcrops, and there are closed depressions up to a few metres in diameter from which the weathering products have been removed, presumably by wind action.

Chemistry of sediment and salt efflorescences

The greatest conductivity and concentrations of calcium, chlorine, magnesium, potassium and sodium occurs along the upwind (eastern) shorelines of Broknes and Mirror Peninsula (Fig. 1). Much lower abundances lie inland in Broknes. A similar trend exists along the upwind shoreline of Stornes (Fig. 1). Broknes is typically 3–5 times saltier than Stornes. Twelve minerals were identified in the 57 efflorescence samples analysed (Figs 3 & 4, Supplementary Table 3 - see www.journals.org/jid_ANS). Most efflorescences were polymineralic, with up to four minerals identified in a single sample. The most abundant salt on northern and eastern Broknes and Mirror Peninsula is halite, with subordinate thenardite. These were identified as being of a marine origin (Fig. 3; Gore *et al*. 1996). Crusts of aragonite or calcite,

Table II. AMS and ^{10}Be results for Larsemann Hills bedrock samples.

Lab code	Sample name	$^{10}Be/^{9}Be$ (x 10^{-15}) (1)	Sample mass (g)	Be carrier mass (mg) (2)	^{10}Be concentration (x 10^{3} atoms g^{-1}) (3)	Altitude (m a.s.l.)	Scaling factor (4)	Site production rate (at/g/yr) (5)
Broknes								
B0449_247	LH-01-97	268.4 ± 23.4	29.75	0.763	459 ± 41	80	1.351	6.61
B0450_248	LH-02-97	232.9 ± 23.3	31.04	0.804	403 ± 41	65	1.329	6.51
B0447_249	LH-03-97	148.3 ± 7.2	26.34	0.758	285 ± 15	115	1.402	6.86
B0451_250	LH-04-97	87.6 ± 7.1	21.00	0.781	218 ± 18	115	1.402	6.86
B0448_258	LH-12-97	293.7 ± 26.3	73.35	0.723	193 ± 18	20	1.266	6.20
B0452_259	LH-13-97	1100 ± 81	62.63	0.727	853 ± 66	22	1.269	6.21
B0627_336	LH-14-97	181.2 ± 10.5	39.60	0.532	163 ± 10	28	1.277	6.25
Stornes								
B0558_252	LH-06-97	72.7 ± 7.3	10.23	0.355	169 ± 17	110	1.394	6.83
B0439_253	LH-07-97	186.9 ± 15.9	16.59	0.668	503 ± 44	110	1.394	6.83
B0529_254	LH-08-97	255.3 ± 10.3	57.30	0.711	212 ± 10	115	1.402	6.86
B0530_255	LH-09-97	211.7 ± 12.3	55.49	0.752	192 ± 12	110	1.394	6.83
B0531_256	LH-10-97	18.1 ± 3.5	35.50	0.726	25 ± 5	40	1.294	6.34
B0532_257	LH-11-97	32.6 ± 3.7	20.34	0.736	79 ± 9	75	1.344	6.58

(1) Final AMS isotopic ratio determined after chemistry blank subtraction and normalization to AMS standards in use at the ANTARES AMS facility [NIST-3425 for $^{10}Be/Be$, nominal value = 30 200 x 10^{-15} (Fink & Smith 2007)]. Blanks prepared from commercially purchased 1000 ppm Be and Al standard solutions. Independent AMS measurements ($n > 3$ repeats) were combined as weighted means with the larger of the total statistical error or mean standard error.

(2) Be carrier determined by mass from an ICP (MERCK) calibration solution at 1000 ± 3 ppm (mg L^{-1}).

(3) Concentrations at site location. Uncertainty represents quadrature addition of 1σ errors in final AMS isotope ratio, masses and a 2% systematic variability in repeat measurement of AMS standards.

(4) Altitude and latitude scaling factors, including modifications for Antarctic pressure-altitude relationship, from Stone (2000).

(5) Production corrections for sample thickness assuming all samples were 4–5 cm using density $\rho = 2.7$ g cm^{-3} and a cosmic ray mean attenuation path length $\Lambda = 150$ g cm^{-2}. Corrections for horizon shielding, and palaeogeomagnetic field variations at 69.3° S (sample site) were not required. Correction for seasonal snow cover not included. Site production rate based on sea level, high latitude spallogenic plus muon (2.5%) production rates of $^{10}Be = 5.1 \pm 0.3$ atoms/g.y and $^{26}Al = 31.1 \pm 1.9$ atoms/g.y from Stone (2000).

https://doi.org/10.1017/S0954102009002028 Published online by Cambridge University Press

Table III. *In situ* cosmogenic ^{10}Be exposure ages.

Field code	Inferred rock surface lowering since deglaciation (mm) (1)	Distance from modern ice sheet edge (km)	^{10}Be max erosion rate (mm ka^{-1}) (2)	^{10}Be exposure age* (ka BP) Scenario 1: no surface lowering (3)	Scenario 2: constant surface lowering	Scenario 3: late surface lowering
LH-01	200	2.7	7.7 ± 0.9	70.1 ± 7.8	83	100
LH-02	10	2.3	8.7 ± 1.1	62.4 ± 7.5	63	64
LH-03	25	1.7	13.1 ± 1.1	41.6 ± 3.4	43	43
LH-04	15	1.7	17.3 ± 1.8	31.8 ± 3.3	32	33
LH-12	100	1.9	17.5 ± 2.0	31.1 ± 3.5	34	37
LH-13	10	2.1	21.1 ± 1.9	140.2 ± 14.2	141	143
LH-14	200	1.9	3.8 ± 0.4	25.9 ± 2.3	31	37
LH-06	?	4.2	22.2 ± 2.7	24.7 ± 3.0	nd	nd
LH-07	100	4.2	7.3 ± 0.8	74.6 ± 8.1	81	89
LH-08	?	4.7	17.7 ± 1.4	30.9 ± 2.4	nd	nd
LH-09	30	4.7	19.5 ± 1.7	28.1 ± 2.5	29	30
LH-10	0	3.9	142.7 ± 30.3	3.9 ± 3.8	4	4
LH-11	0	3.6	46.1 ± 6.2	11.9 ± 1.6	12	12

* Errors are 1 σ. It is assumed that there is no inheritance of cosmogenic nuclides. nd = no data.
(1) Measured height difference between sampled bedrock and adjacent striated surface (which was not sampled).
(2) Maximum model erosion rate assuming measured ^{10}Be concentration has reached erosional equilibrium.
(3) Minimum model exposure ages based on ^{10}Be half-life = 1.51 Ma and zero erosion rate. Exposure ages errors propagated from concentrations with additional errors of 7% in production rate.

identified as subglacial precipitates, occur to the south of Lake Nella. Salt efflorescences on Stornes, although scarcer than on Broknes, were similarly dominated by halite, but with subordinate authigenic rock weathering products.

^{14}C dating of mumiyo

Mumiyo was obtained from five locations from Three Man Peak, the nest sites occurring under scree blocks and in tafoni hollows, the formation of which must predate occupation by the petrels. AMS radiocarbon dating of the basal 2 mm of these five samples yielded radiocarbon (uncorrected, uncalibrated) ages of 2.7–1.5 ^{14}C ka BP (Table I). Modern samples of marine shell and marine algae from Vestfold Hills yielded ages of 950 a BP and 1310 a BP respectively (Adamson & Pickard 1983, 1986) due to ^{14}C depletion of oceanic waters and the food chain (the marine reservoir effect; Ascough *et al*. 2005). However, a very recent age of only 500 years has been obtained from the base of a mumiyo accumulation 18 cm thick in Vestfold Hills (Kiernan *et al*. 2003), indicating that a robust correction factor for mumiyo requires further investigation. As a consequence, the true age of the mumiyo remains uncertain and radiocarbon years are reported here. Nevertheless, they provide a useful indication that the tafoni and scree have been stable on a 1 ka timescale, which is significant in considering likely rates of weathering and erosion in this environment.

Exposure age dating

The ^{10}Be concentrations and exposure ages were calculated assuming zero weathering, and using the amount of lowering referenced from striated surfaces nearby (Tables II & III, Fig. 5, Supplementary Tables 1 & 2 - see www.journals.org/jid_ANS). The three samples with scenario ages exceeding 1 σ (Table III) are likely to have been affected by post-exposure weathering and erosion. The exposure ages from Broknes uncorrected for surface weathering show a

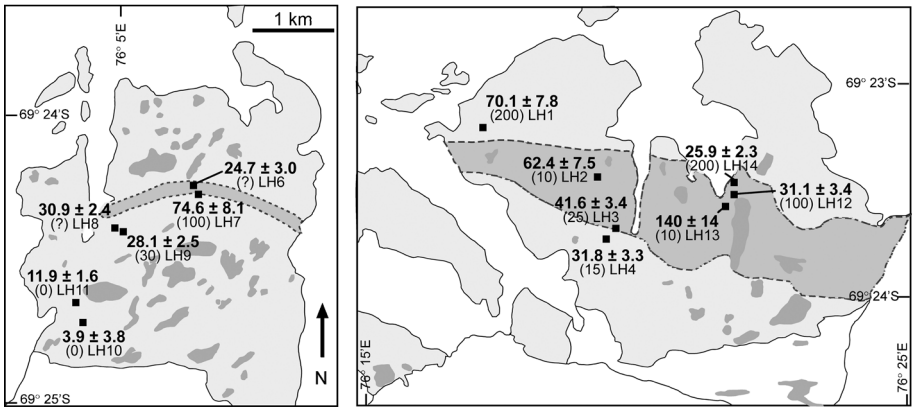

Fig. 5. Cosmogenic nuclide exposure ages ± 1 σ error. The quoted ages are for weathering scenario (1), which assumes that postglacial lowering has no effect on ^{10}Be concentration. Numbers in brackets refer to the depth of postglacial weathering of the rock surface (in mm).

https://doi.org/10.1017/S0954102009002028 Published online by Cambridge University Press

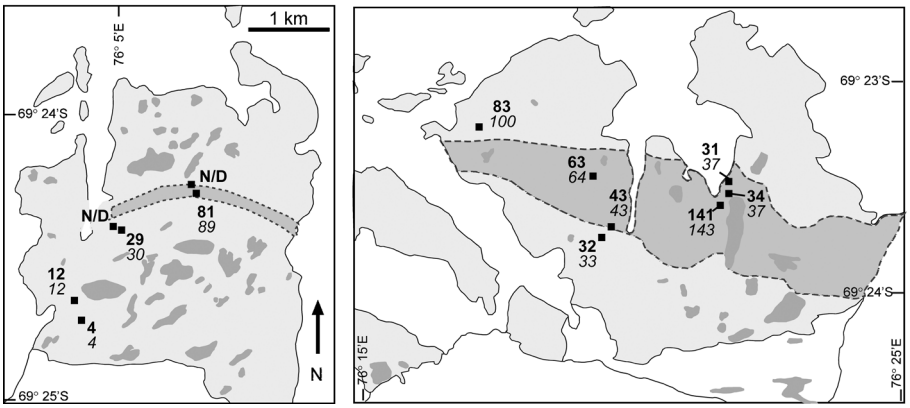

Fig. 6. Cosmogenic nuclide exposure ages (in ka) following correction for the amount of postglacial erosion as indicated by field relationships, and detailed in Fig. 5. Bold numbers refer to postglacial erosion for scenario (2), where erosion is constant following deglaciation. Numbers in italics are for scenario (3), where all erosion occurs just prior to the present day. N/D = not determined.

complex pattern that is glaciologically inconsistent, with age reversals with respect to distance from the ice sheet. Corrected for surface lowering, the Broknes samples young toward the ice sheet with exposure ages of > 100 ka in the northern parts of the peninsula and > 30 ka in the centre of the peninsula (Fig. 6). The uncorrected exposure ages on Stornes are consistent, younging toward the ice dome at the south of the peninsula. Corrected for surface lowering, the northern part of the peninsula was probably exposed prior to 100 ka BP, with the central part of the peninsula exposed prior to the Last Glacial Maximum. Within 1–2 km of Stornes ice dome, exposure from the ice occurred around the start of the Holocene 10 ka BP.

Discussion

The widespread occurrence of ice-eroded landforms, glacial striae (albeit rare) on hilltops, diamictons and moraines near to the present day coast demonstrate that the East Antarctic ice sheet formerly covered Larsemann Hills, however a robust deglaciation chronology has not been established. The preservation of old interglacial lacustrine sediments suggests continuous exposure of Broknes through the last glacial cycle (Hodgson *et al*. 2001, 2005, Squier *et al*. 2005, Cromer *et al*. 2006), but until now confirmation of this interpretation has been hindered by the lack of an appropriate absolute age dating technique.

The marked contrast in weathering between rock surfaces above and below the Holocene marine transgression implies that the higher, more weathered rock surfaces are probably considerably older than the Holocene. Similarly, the mumiyo ^{14}C ages obtained from snow petrel nests in boulder accumulations and tafoni hollows show that the nesting shelters have undergone little change in the 2.0–1.5 ka since they were first colonized, indicating that these post-glacial weathering forms in central and northern Broknes are of considerable age. If the contemporary rock-surface lowering rate of 0.015 mm a^{-1} over a six year period (Spate *et al*. 1995) is applicable over long periods, then ~150 mm of rock could be lost over 10 ka and 1.5 m over 100 ka. The latter extrapolation is in the order of the depth of some tafoni pits on rock benches and the heavily weathered hill flanks in Larsemann Hills. This has significant implications for interpretation of the cosmogenic nuclide exposure ages. Given potential rock-surface lowering rates of ~1.5 m 100 ka^{-1}, much of the cosmic ray irradiated layer could be removed from bedrock exposed to subaerial weathering during the last glacial cycle. Hence, a significant underestimate of the age of deglaciation may result if simple interpretations of the exposure ages alone are made.

Broknes exhibits a diffuse chemical boundary, or "salt line" (Adamson & Pickard 1986, Gore *et al*. 1996), ~750 m wide which separates the salt-rich northern and eastern areas from the less salty southern and western areas (Figs 2 & 3). Field observations of rock weathering and measurements of sediment geochemistry indicate that Stornes also exhibits a thin and poorly defined salt line, with an enhanced addition of salts in the north-eastern corner of the peninsula. These chemical contrasts between the north-eastern and south-western areas of the peninsulas have developed in response to long-term subaerial exposure of the land to sea spray from the dominant ESE wind. The strong contrast in saltiness between Broknes and Stornes results from the frequency of occurrence of ice-free water in the upwind direction. The sea ice in front of Dalk Glacier, to the east of Broknes and Mirror Peninsula, breaks out most years and open sea water typically exists immediately upwind of the salty land areas, allowing sea spray to deposit onto the land. In contrast, the sea ice upwind (east) of Stornes is pinned in by grounded icebergs and small islands and rarely breaks out, and so the wind typically blows over sea ice and transports snow drift rather than salty sea spray. The halite and thenardite salt enhancement that results has created a chemical and rock weathering contrast both between Stornes and Broknes, and within Broknes. Salt weathering, which enhances single grain disaggregation (Williams & Robinson 1981, Jerwood *et al*. 1990), has created strong contrasts in the weathering of rock and sediment which are consistent with this simple chemical model.

https://doi.org/10.1017/S0954102009002028 Published online by Cambridge University Press

The terrestrial cosmogenic nuclide exposure age data presented in this paper support the interpretation of last deglaciation of the northern parts of Larsemann Hills sometime prior to 100 ka BP, with exposure of the central areas prior to Last Glacial Maximum, and a small Late Glacial/early Holocene retreat of the ice edge to its present position. The strongly weathered nature of the bedrock made application of the exposure age method challenging in places, because any process which removes the rock also removes cosmogenic nuclides, leading to underestimates of the true age of deglaciation. This effect is enhanced with sites that have been subaerially exposed for a long period, or where the lowering of the rock surface is accelerated by processes such as salt-enhanced weathering. We have applied a correction for surface lowering, based on detailed field observations which revealed the extent of surface lowering at each site since deglaciation. It is also possible, however, that there has been some inheritance of ^{10}Be if the last glaciation of Larsemann Hills was short-lived or not strongly erosive, causing less than ~1.5 m of bedrock lowering. We cannot investigate this notion further without additional sample collections and investigations, although this should be considered a priority for subsequent research. The single isotope dataset presented here, corrected for rock surface erosion, is consistent with a simple ice retreat scenario, the rock weathering observations and extrapolations, and the existing ^{14}C and OSL chronologies and interpretations of a Last Interglacial deglaciation (Hodgson *et al*. 2001, 2005, 2006, Squier *et al*. 2005, Cromer *et al*. 2006). The weathering and chemical boundary defined as the salt line (Fig. 1), is more consistent with the flux of salt-laden sea spray than a former glacial limit.

The Broknes results are consistent with the radiocarbon age of 24 950 ± 710 ^{14}C yr BP (ANU 8826; Burgess *et al*. 1994) and an optically stimulated luminescence age (20 710 ± 1769 BP; Hodgson *et al*. 2001), but a much greater age of 140.2 ± 14.2 ka was also obtained here. The latter came from an outcrop of particularly resistant rock closer to present ground level and might be due either to insufficient glacial erosion having occurred with a resultant failure to remove cosmogenic nuclides formed during prior subaerial exposure, or by less susceptibility to postglacial subaerial weathering and erosion. The very heavily weathered condition of the nearby moraine at Lake Reid suggests that this trough has not been glaciated for a very long time. A date of 43 800 ^{14}C yr BP has previously been obtained from lacustrine sediments in Lake Reid, ~2.5 km from the present ice edge, and another of 44 400 ^{14}C yr BP from sediments in Progress Lake, only a few hundred metres from the edge of the Dalk Glacier (Hodgson *et al*. 2001).

The Stornes data show deglaciation of the hilltops occurred substantially earlier than the mid–late Holocene age suggested by the radiocarbon-based lacustrine sediment chronologies of Gillieson (1991) and Hodgson *et al*. (2001). The exposure ages are consistent with the continuous exposure of Kolloy, an island 4.5 km further to the north, for at least 40 ka, as inferred by Hodgson *et al*. (2001) on the basis of a basal radiocarbon date of > 43 200 ^{14}C yr BP from Kirisjes Pond. Glaciation of Kirisjes Pond, like Lake Nella and Progress Lake on Broknes, would have required substantial expansion of the ice sheet because the Dalk Glacier trough is likely to have deflected smaller increases in ice discharge around the hills.

The three oldest mumiyo dates are identical, implying simultaneous colonization of the nest sites ~2.5 ka BP. Fluctuations in late Holocene climate or sea ice extent may have influenced the timing of this occupation. Verleyen *et al*. (2004) recognized a warm period from 7400–5230 cal yr BP followed by a return to conditions similar to now until 2750 cal yr BP when there was a brief return to stratified open water conditions and reduction in near-shore sea ice until 2200 cal yr BP. Lake water and salinity depths suggest conditions were warm and moist from *c*. 3000–2000 cal yr BP after which conditions became drier (Verleyen *et al*. 2004).

Conclusions

Widespread glacially-eroded landforms and diamictons indicate that Larsemann Hills has previously been entirely glaciated by the East Antarctic ice sheet. Terrestrial cosmogenic nuclide dating indicates that the last deglaciation of Broknes occurred no more recently than early in the last glacial cycle. Eleven of our ^{10}Be ages indicate that extensive glaciation did not occur in Larsemann Hills during the LGM and four suggest the area was probably not glaciated at any time during the last glacial cycle. A single date of 140 ka raises the possibility that Larsemann Hills have not been glaciated since MIS 6. Salt-enhanced subaerial weathering results in exposure ages that in places are underestimates, suggesting that 100 ka is a minimum for the true deglaciation age. This finding is consistent with evidence from lake sediments which were used to suggest that Broknes was exposed throughout much of the last glacial cycle (Hodgson *et al*. 2001, 2005, Cromer *et al*. 2006). However, Stornes was deglaciated earlier than suggested by Hodgson *et al*. (2001), which implies that the ice sheet has remained even more stagnant during the Last Glacial Maximum than hitherto recognised.

Acknowledgements

We thank the Australian Antarctic Division (ASAC 1118), Australian Research Council (DP0556728) and Australian Nuclear Science and Technology Organisation (CcASH Project 0203v) for logistic and financial support. For helpful discussion or assistance in the field or laboratory, we thank Andrew Baird, Dennis Branch, Jim Burgess,

Eric Colhoun, Peter Corcoran, Dudley Creagh, Jessica Lawrence and Andy Spate. We thank the referees, Prof W.B. Lyons and Dr E. Colhoun for comments which improved the manuscript.

References

Adamson, D.A. & Pickard, J. 1983. Late Quaternary ice movement across the Vestfold Hills, East Antarctica. *In* Oliver, R.L., James, P.R. & Jago, J.B., *eds*. *Antarctic earth science*. Canberra: Australian Academy of Science, 465–469.

Adamson, D.A. & Pickard, J. 1986. Cainozoic history of the Vestfold Hills. *In* Pickard, J., *ed*. *Antarctic oasis: terrestrial environments and history of the Vestfold Hills*. Sydney: Academic Press, 63–97.

Ascough, P., Cook, G. & Dugmore, A. 2005. Methodological approaches to determining the marine radiocarbon reservoir effect. *Progress in Physical Geography*, **29**, 532–547.

Bien, L., Xue, Z., Lu, L., Lu, C., Jia, P. & Zhang, Y. 1994. *Surface meteorological data at Zhong Shan Station, Antarctica 1989–1992*. CHINARE Data Report 7 (Meteorology 6). Shanghai: Polar Research Institute of China, 159 pp.

Burgess, J.S., Spate, A.P. & Shevlin, J. 1994. The onset of deglaciation in the Larsemann Hills, eastern Antarctica. *Antarctic Science*, **6**, 491–495.

Carson, C.J., Dirks, P.G.H.M., Hand, M., Sims, J.P. & Wilson, C.J.L. 1995. Compressional and extensional tectonics in low-medium pressure granulites from the Larsemann Hills, East Antarctica. *Geological Magazine*, **132**, 151–170.

Child, D., Elliot, G., Misfud, C., Smith, A.M. & Fink, D. 2000. Sample processing for earth science studies at ANTARES. *Nuclear Instruments and Method in Physics Research*, **B172**, 856–860.

Cromer, L., Gibson, J.A.E., Swadling, K.M. & Hodgson, D.A. 2006. Evidence for a lacustrine faunal refuge in the Larsemann Hills, East Antarctica, during the Last Glacial Maximum. *Journal of Biogeography*, **33**, 1314–1323.

Dirks, P.H.G.M., Carson, C.J. & Wilson, C.J.L. 1993. The deformational history of the Larsemann Hills, Prydz Bay - the importance of the Pan-African (500 ma) in East Antarctica. *Antarctic Science*, **5**, 179–192.

Fink, D. & Smith, A. 2007. An inter-comparison of ^{10}Be and ^{26}Al AMS reference standards and the ^{10}Be half-life. *Nuclear Instruments and Methods*, **B259**, 600–609.

Fink, D., Hotchkis, M.A.C., Hua, Q., Jacobsen, G.E., Smith, A.M., Zoppi, U., Child, D., Mifsud, C., van der Gaast, H.A., Williams, A.A. & Williams, M. 2004. The ANTARES AMS facility at ANSTO. *Nuclear Instruments and Method in Physics Research*, **B223**, 109–115.

Gillieson, D.S. 1991. An environmental history of two freshwater lakes in the Vestfold Hills, Antarctica. *Hydrobiologia*, **214**, 327–331.

Gore, D.B. 1997. Blanketing snow and ice: constraints on radiocarbon dating deglaciation in East Antarctic oases. *Antarctic Science*, **9**, 336–348.

Gore, D.B., Creagh, D.C., Burgess, J.S., Colhoun, E.A., Spate, A.P. & Baird, A.S. 1996. Composition, distribution and origin of surficial salts in the Vestfold Hills, East Antarctica. *Antarctic Science*, **8**, 73–84.

Hodgson, D.A., Verleyen, E., Squier, A.H., Sabbe, K., Keely, B.J., Saunders, K.M. & Vyverman, W. 2006. Interglacial environments of coastal east Antarctica: comparison of MIS 1 (Holocene) and MIS 5e (Last Interglacial) lake-sediment records. *Quaternary Science Reviews*, **25**, 179–197.

Hodgson, D.A., Verleyen, E., Sabbe, K., Squier, A.H., Keely, B.J., Leng, M.J., Saunders, K.M. & Vyverman, W. 2005. Late Quaternary climate-driven environmental change in the Larsemann Hills, East Antarctica, multi-proxy evidence from a lake sediment core. *Quaternary Research*, **64**, 83–99.

Hodgson, D.A., Noon, P.E., Vyverman, W., Bryant, C.L., Gore, D.B., Appleby, P., Gilmour, M., Verleyen, E., Sabbe, K., Jones, V.J., Ellis-Evans, J.C. & Wood, P.B. 2001. Were the Larsemann Hills ice-free through the Last Glacial Maximum? *Antarctic Science*, **13**, 440–454.

Jerwood, L.C., Robinson, D.A. & Williams, R.B.G. 1990. Experimental frost and salt weathering of chalk - I. *Earth Surface Processes and Landforms*, **15**, 611–624.

Kiernan, K., McConnell, A., Colhoun, E. & Lawson, E. 2003. Radiocarbon dating of mumiyo from the Vestfold Hills, East Antarctica. *Papers & Proceedings of the Royal Society of Tasmania*, **136**, 141–144.

Lal, D. 1991. Cosmic ray labeling of erosion surfaces; *in situ* nuclide production rates and erosion models. *Earth and Planetary Science Letters*, **104**, 424–439.

Spate, A., Burgess, J.S. & Shevlin, J. 1995. Rates of rock surface lowering, Princess Elizabeth Land, eastern Antarctica. *Earth Surface Processes and Landforms*, **20**, 567–573.

Squier, A.H., Hodgson, D.A. & Keely, J. 2005. Evidence of late Quaternary environmental change in a continental east Antarctic lake from lacustrine sedimentary pigment distributions. *Antarctic Science*, **17**, 361–376.

Stone, J.O. 2000. Air pressure and cosmogenic isotope production. *Journal of Geophysical Research*, **B105**, 23 753–23 759.

Stuwe, K., Braun, H.-M. & Peer, H. 1989. Geology and structure of the Larsemann Hills area, Prydz Bay, East Antarctica. *Australian Journal of Earth Sciences*, **36**, 219–241.

Sugden, D.E., Balco, G., Cowdery, S.G., Stone, J.O. & Sass, L.C. 2005. Selective glacial erosion and weathering zones in the coastal mountains of Marie Byrd Land, Antarctica. *Geomorphology*, **67**, 317–334.

Sumner, P.D. 2004. Rock weathering rates on subantarctic Marion Island. *Arctic, Antarctic, and Alpine Research*, **36**, 123–127.

Verleyen, E., Hodgson, D.A., Sabbe, K. & Vyverman, W. 2004. Late Quaternary deglaciation and climate history of the Larsemann Hills, East Antarctica. *Journal of Quaternary Science*, **19**, 361–375.

White, D.A. 2007. *Cenozoic glacial history and landscape evolution of Mac.Robertson Land and the Lambert Glacier-Amery ice shelf system, East Antarctica*. PhD thesis, Department of Physical Geography, Macquarie University, Sydney.

Williams, R.B.G & Robinson, D.A. 1981. Weathering of sandstone by the combined action of frost and salt. *Earth Surface Processes and Landforms*, **6**, 1–9.

Zwartz, D. 1995. *The recent history of the Antarctic Ice Sheet:*constraints *from sea-level change*. PhD thesis, Research School of Earth Sciences, The Australian National University.